Available online www.jsaer.com

***Journal of Scientific and Engineering Research*, 2022, 9(11):111-118**

Research Article

ISSN: 2394-2630
CODEN(USA): JSERBR

The effect of irradiation energy on the electrical parameters of a monofacial silicon solar cell in dynamic frequency regime under monochromatic illumination

El hadji Ndiaye*, Fatimata Ba, Seydou Faye, Mor Ndiaye, Issa Diagne

*Laboratory of Semiconductors and Solar Energy, Physics Department, Faculty of Science and Technology, University Cheikh Anta Diop, Dakar, Senegal

Abstract In this work, we study the influence of the irradiation energy on the electrical parameters of a monofacial solar cell in frequency dynamic regime under monochromatic illumination. After solving the minority charge carrier continuity equation in the presence of irradiation energy, we establish new expressions for the minority charge carrier density and electrical parameters such as photocurrent density, photovoltage and dynamic impedance. Starting from these equations, we have represented the profiles of some electrical parameters finally to highlight the effect of the irradiation energy on the latter.

Keywords Monofacial silicon solar cell, frequency modulation, irradiation energy, electrical parameters

1. Introduction

Given the relatively high cost of photovoltaic cells, in recent years, an intense effort has been continuously made to optimize the performance of photovoltaic systems. It is in this context that many avenues of research are explored: improvement of manufacturing processes, better use of all the wavelengths of the solar spectrum, use of concentrators using mirrors and lenses to focus the radiation on the photovoltaic cell, improve efficiency by combining amorphous and crystalline silicon in the same photovoltaic cell [1,2]. Indeed, from theoretical studies, we propose in this article, the influence of the irradiation energy on the electrical parameters of a monofacial silicon solar cell under monochromatic illumination in a dynamic frequency regime.

2. Theory

The solar cell considered is of the n+pp+ type and its structure is presented in figure 1.

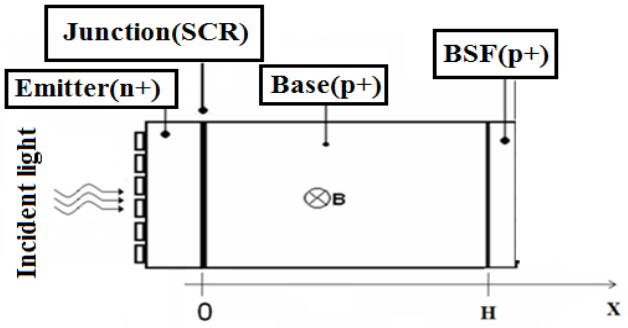

Figure 1: An n+-p-p+ structure of a silicon solar cell

Under the effect of excitation (optical or electrical), charge carriers are generated in the base of the solar cell. The carriers thus generated can either cross the space charge zone where they participate in the external current, or they undergo surface or volume recombinations. These are due to defects (grain boundaries, uncontrolled impurities, dislocations, etc.) related to the manufacture of the solar cell. Taking into account the phenomena of generation, recombination and diffusion within the solar cell, the continuity equation of the minority charge carriers in the base at the abscissa x in frequency dynamic regime is of the form:

$$\frac{\partial^2\delta(x,t)}{\partial x^2}-\frac{1}{D}\frac{\partial\delta(x,t)}{\partial t}-\frac{\partial\delta(x,t)}{D\tau}=\frac{G(x,t)}{D} \quad (01)$$

Where is the density of electrons generated in the base at depth x in the base, [3] is the diffusion coefficient, [4] the overall carrier generation rate, and [5] the carrier lifetime. For the resolution of the continuity equation, the global generation rate and the density of the minority carriers can be put respectively in the following form.

$$\delta(x,t)=\delta(x)\exp(j\omega t) \quad (02)$$

$$G(x,t)=g(x)\exp(j\omega t) \quad (03)$$

$$g(x)=\varphi_l\alpha_t\left(1-R_t\right)\exp\left(-\alpha_t x\right) \quad (04)$$

The expressions of the diffusion coefficient and of the diffusion length as a function of the irradiation energy and of the damage coefficient kl in the dynamic frequency regime are given respectively by the following equations [6]

$$D^*\left(\omega,Kl,\varphi_p,B\right)=D\left(Kl,\varphi_p\right)\frac{\left[1+\tau^2\left(\omega_c^2+\omega^2\right)+j\omega\tau\left[\tau^2\left(\omega_c^2-\omega^2\right)-1\right]\right]}{4\tau^2\omega^2+\left[1+\tau^2\left(\omega_c^2-\omega^2\right)\right]^2} \quad (05)$$

Avec

$$D\left(kl,\varphi_p\right)=\frac{L\left(kl,\varphi_p\right)^2}{\tau} \quad (06)$$

$$L\left(K_l,\varphi_p\right)=\frac{1}{\sqrt{\frac{1}{L_0^2}+K_l\varphi_p}} \quad (07)$$

$$L_0=\sqrt{D_0\tau} \quad (08)$$

$$L\left(Kl,\varphi_p,\omega\right)=L\left(kl,\varphi_p\right).\sqrt{\frac{1-j.\omega.\tau}{1+\left(\tau.\omega\right)^2}} \quad (09)$$

$D\left(Kl,\varphi\right)$ is the diffusion coefficient depending on the damage coefficient and the irradiation flux.

$L\left(Kl,\varphi\right)$ is the scattering length as a function of the damage coefficient and the irradiation flux.

L0 is the scattering length in the absence of pulsation, irradiation and magnetic field.

D0 is the diffusion coefficient in the absence of pulsation, irradiation and magnetic field

$L(Kl,\varphi,B)$ is the scattering length as a function of the damage coefficient, the irradiation flux and the magnetic field.

Thus equation (1) can be put in the form:

$$\frac{\partial^2(x)}{\partial x^2}-\frac{1}{L^2(\omega)}\partial(x)=-\frac{g(x)}{D^*} \quad (10)$$

The equation (04) being a differential of the second degree with second member therefore the general solution is:

$$\delta(x)=A\cosh\left(\frac{x}{L}\right)+B\sinh\left(\frac{x}{L}\right)-\frac{\alpha I_0(1-R)L^2}{D(\alpha^2L^2-1)}\exp(-\alpha x) \quad (11)$$

To determine the coefficients A and B, the following boundary conditions [7] are used.

At the junction (x = 0) $$\frac{\partial\delta(0)}{\partial x}=\frac{Sf}{D^*}\delta(0) \quad (12)$$

On the back side (= H) (x = H) $$\frac{\partial\delta(H)}{\partial x}=-\frac{Sb}{D^*}\delta(H) \quad (13)$$

Where, Sf and Sb are the recombination rates of the minority charge carriers at the junction and at the back face, respectively; H the thickness of the base. Sf is the sum of two contributions [8]

$$Sf = Sf_0 + Sf_j \quad (14)$$

Sf0 is known as the intrinsic recombination rate at the junction induced by the shunt resistor and Sfj is the recombination rate related to the load imposing the operating point on the solar cell.

3. Results and Discussions

3.1 Generation rate profile as a function of wavelength

The generation rate of minority carriers is given by equation (4). Its profile is shown in Figure 2 as a function of wavelength.

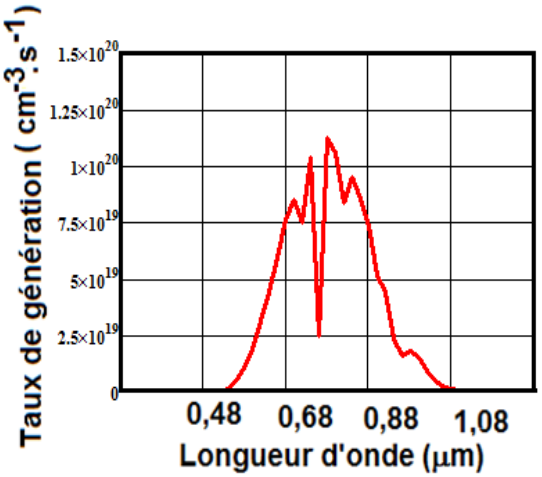

Figure 2: Generation rate as a function of wavelength.
x=0.001cm.

On this curve, we notice that the generation rate increases with short wavelengths and gradually decreases in the case of long wavelengths. Indeed, with small wavelengths, we have a large absorption unlike with long wavelengths. This is how, for the rest of our work, we will take a wavelength located in the short wavelength zone.

3.2 Profile of the diffusion coefficient as a function of the pulsation

We represent in Figure 3 the profile of the diffusion coefficient as a function of the logarithm of the frequency for different values of the magnetic field.

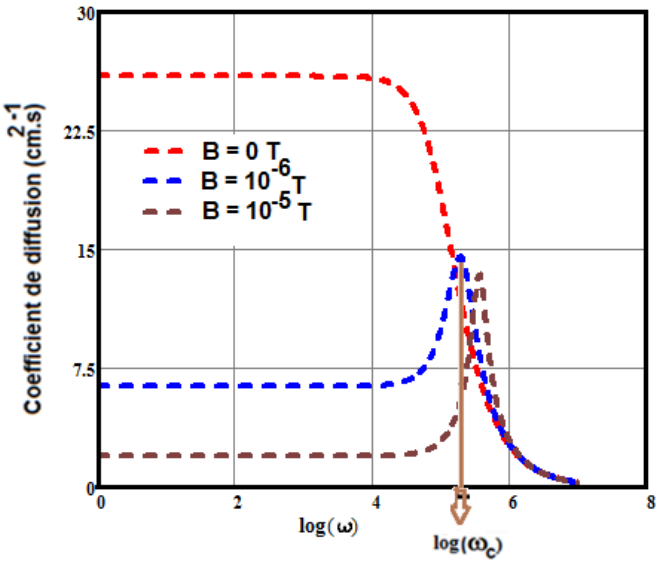

Figure 3: Modulus of the diffusion coefficient as a function of the logarithm of the pulsation. Kl=10 MeV^{-1}.s^{-1}

Graphically, we find that $\omega_C = 10^{5.2}$ *rad.S^{-1}*

From this figure, we notice that the modulus of the diffusion coefficient is constant in quasi-static regime. However, as soon as we are in the dynamic frequency regime, we observe that the diffusion coefficient increases gradually up to a certain value of the so-called cyclotron frequency noted ωc [9], where we observe resonance peaks. This is how we made the choice of ωc as the value to be fixed for the frequency in the rest of the work.

3.3 Photocurrent Density

The photocurrent density is the photocurrent reported at the surface of the solar cell. It is due to the diffusion of minority charge carriers across the junction. Knowing the expression for the minority carrier density, we can determine the expression for the photocurrent density using FICK's law. It is given by the following relationship:

$$J(Sf,Sb,\lambda,\omega,kl,\varphi,B) = q.D.\left.\frac{\partial\delta(x,Sf,Sb,\lambda,\omega,kl,\varphi_p,B)}{\partial x}\right|_{x=0} \qquad (15)$$

The photocurrent density profile is shown in Figure 4 as a function of the recombination velocity at the Sf junction for different values of irradiation energy.

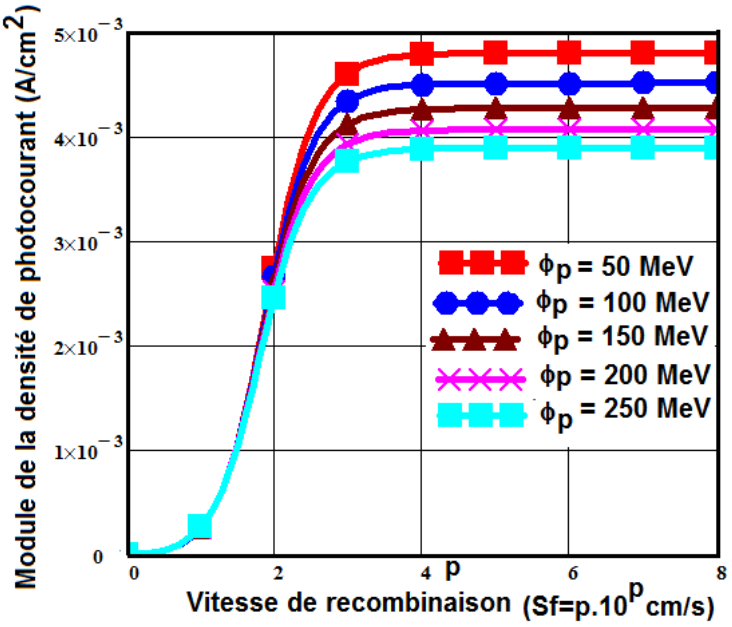

Figure 4: Modulus of photocurrent density as a function of recombination velocity for different values of irradiation energy Kl=10 MeV^{-1}.s^{-1} ; λ=0.6μm; B= 10^{-6} T; ω =105.2 rad.S^{-1}

Note that the photocurrent increases with the recombination rate Sf and has two levels: one at low values of Sf and the other at high values of Sf. The first level reflects an open-circuit situation while the second corresponds to to the short-circuit of the solar cell. Increasing the recombination rate at the junction allows maximum minority charge carriers to cross the junction and participate in the photocurrent. There is a remarkable decrease in the short-circuit photocurrent density when the irradiation energy increases. Indeed, the irradiation energy decreases the mobility of the carriers. Thus there will be fewer or fewer charges in the base to participate in the photocurrent.

3.4 Study of photovoltage

When the solar cell is lit, a photovoltage V appears across it, the expression of which is given by the Boltzmann relationship:

$$V = V_T \ln\left(\frac{N_b}{n_i^{\,2}}\delta(0) + 1\right) \tag{16}$$

Where Nb is the doping level of the base (N_b=5.10^{17} cm^{-3}) ni is the intrinsic density of the minority carriers ni=1010cm^{-3}.

VT the thermal tension defined by the following relationship:

$$V_T = \frac{K.T}{q} \tag{17}$$

Knowing that :

K the Boltzmann constant.

q the charge of the electron.

T the absolute temperature at thermal equilibrium (T=300K).

The profile of the phototension as a function of the recombination speed for different values of the irradiation energy, is represented in figure 5

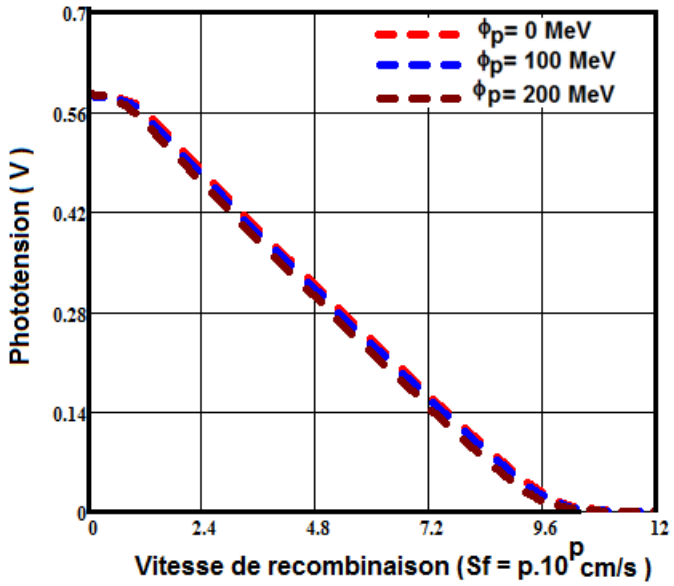

Figure 5: Modulus of the phototension as a function of the recombination rate for different values of the irradiation energy. Kl=10 MeV^{-1}.s^{-1} ; λ=0.6μm; B= 10^{-6} T; ω =105.2 rad.S^{-1}

The photovoltage is maximum in open circuit. On the other hand, in short-circuit, the photovoltage is minimal and becomes asymptotic if Sf is greater than 1011 cm/s. The maximum photocurrent is obtained. This empties the base of its carriers, thus causing the phototension to drop. It is also noted that the increase in the irradiation energy leads to a decrease in the phototension due to the reduction of the minority carriers by the irradiation energy.

3.5 Study of dynamic impedance

The dynamic impedance **[10]** is given by the following relationship:

$$Z(Sb,\lambda,\omega,Kl,\varphi p,B)=\frac{V_{CO}(Sb,\lambda,\omega,Kl,\varphi p,B)}{J_{CC}(Sb,\lambda,\omega,Kl,\varphi p,B)} \quad (18)$$

For the continuation, we will represent the diagrams of Nyquist and the diagrams of Bode [11] of the dynamic impedance finally to give the impact of the energy of irradiation on this quantity.

3.5.1 Bode diagram of impedance.

The Bode plot is a method developed to simplify obtaining frequency response plots. As part of our study, we will plot the Bode diagrams of the phase of the impedance as a function of the logarithm of the angular frequency.

Figure 6 represents the phase profile of the impedance as a function of the logarithm of the pulsation for different values of the irradiation energy.

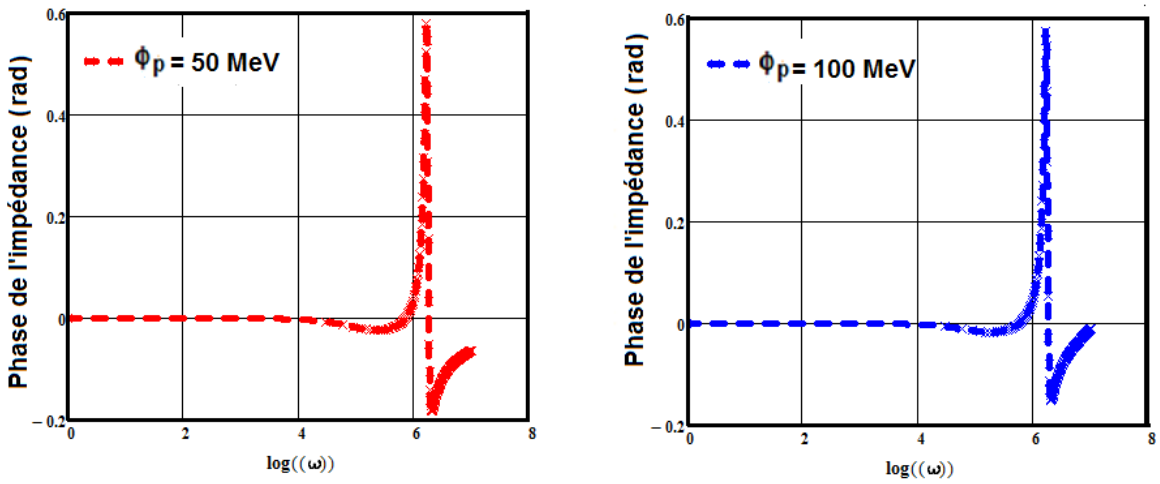

Figure 6: Variation of the phase of the impedance as a function of the frequency for different values of the irradiation energy. Kl=10 $MeV^{-1}.s^{-1}$; λ=0.6μm; B= 10^{-6} T

The Bode representation of the phase of the impedance as a function of the logarithm of the frequency, first shows that there is a frequency below which the phase is zero. In this zone, the inductive and capacitive phenomena compensate each other: this is resonance. Then, when we are in frequency dynamic regime, we observe that the phase is negative first, which shows the capacitive effects, then the phase becomes positive confirming the inductive effects of the impedance.

3.5.2 Nyquist diagram of impedance.

The Nyquist diagram is the representation of the imaginary part versus the real part of the complex function. In Figure 7, we represent the profile of the imaginary part as a function of the real part of the dynamic impedance for different values of the irradiation energy.

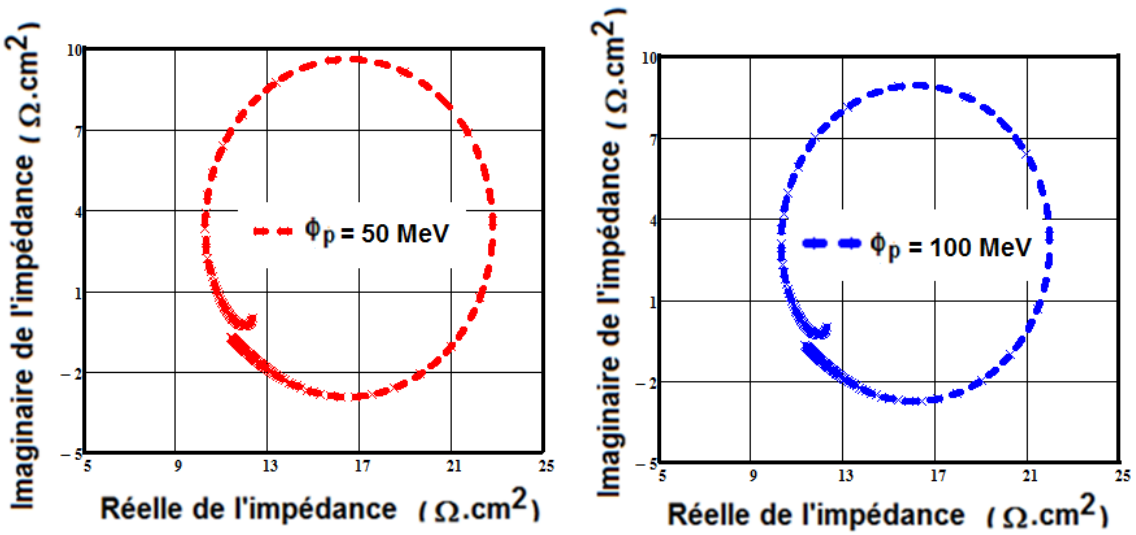

Figure 7: Imaginary part of the impedance as a function of the real part for different values of the irradiation energy.Kl=10 $MeV^{-1}.s^{-1}$; λ=0.6μm; B= 10^{-6} T

The Nyquist diagram of dynamic impedance for different values of irradiation energy is shown in Fig. These curves are circular with positive and negative values of the imaginary part of the impedance which would justify the inductive and capacitive effects mentioned above.

Table 1: Parallel and series resistance values as a function of irradiation energy

ϕ_p(MeV)	Rp ($\Omega.cm^2$)	Rs ($\Omega.cm^2$)
50	12.06	10.27
100	11.61	10.32
150	8.99	8.24
200	8.53	8.20
250	8.14	8.10

From this table, we find that when the value of the irradiation energy increases, the resistance RP decreases which is due to the slowing down of the diffusion of the minority carriers caused by the irradiation. Consequently, the performance of the solar cell decreases; this implies a drop in the conversion efficiency of the solar cell.

4. Conclusion

In this article, we studied the electrical parameters such as: photocurrent density, photovoltage and dynamic impedance. In most cases, we have highlighted the effects of phenomenological parameters such as the recombination rate at the junction and then of the macroscopic parameter which is the irradiation energy. This study showed the influence of irradiation on all of these quantities considered, in particular the negative effects of the degradations caused by irradiation. Indeed, the irradiation energy decreases the performance of the solar cell by reducing the efficiency of the solar cell.

References

[1]. http://www.vent-de-soleil.com/energie_solaire/accueil_energie_solaire.html

[2]. http:// fr.wikipedia.org/wiki/Cellule_photovoltaïque

[3]. Sontag, D., Hahn, G., Geiger, P., Fath, P. and Bucher, E. (2002) Two-Dimensional Resolution of Minority Carrier Diffusion Constant in Different Silicon Materials. Solar Energy Materials & Solar Cells, 72, 533-539.

[4]. Zoungrana, M., Zerbo, I., Sere, A., Zouma, B. and Zougmore, F. (2009) 3D Bifacial Study of Silicon Solar Cell under Intense Light Concentration and under External Magnetic Field Constant. *Global Journal of Engineering Research*, 10,113-124.

[5]. Ahmed, F. and Garg, S. (1986) International Centre for Theoretical Physics (ICTP), Internal Report. Trieste, August.

[6]. Amadou Diao, Ndeye Thiam, Martial Zoungrana, Gokhan Sahin, Mor Ndiaye, Grégoire Sissoko. (2009) Diffusion Coefficient in Silicon Solar Cell with Applied Magnetic Field and under Frequency: Electric Equivalent Circuits. World Journal of Condensed Matter Physics, 4, 2014.

[7]. Sissoko, G., Museruka, C., Correa, A., Gaye, I. and Ndiaye, A.L. (1996) Spectral Light Effect on Recombination Parameters of Silicon Solar Cell. *Proceedings of World Renewable Energy Congress*, Part 3, Denver, 15-21,1487-1490.

[8]. Sissoko, G., Correa, A., Nanema, E., Diarra, M.N., Ndiaye, A.L. and Adj, M. (1998) Recombination Parameters Measurement in Sijicon Double Sided Surface Field Cell. Proceedings of the World Renewable Energy Conference, Florence, 20-25 September 1998, 1856-1859.

[9]. Introduction à la Physique de L'état solide '' C. Kittel, pp. 284 – 285.

[10]. A.J. Steckl and S.P. Sheu (1979) Solid. State Electronics Vol. 23, 21, 715 – 720

[11]. Lathi, Bhagwandas Pannalal: Signals, Systems and Controls.